Available online at www.sciencedirect.com

ScienceDirect

Procedia Computer Science 232 (2024) 1212–1221

Procedia Computer Science

www.elsevier.com/locate/procedia

5th International Conference on Industry 4.0 and Smart Manufacturing

Surface quality related to machining parameters in 3D-printed PETG components

Mohamad El Mehtedi*, Pasquale Buonadonna, Rayane El Mohtadi, Francesco Aymerich, Mauro Carta

DIMCM, University of Cagliari, Via Marengo 2, Cagliari, 09123, Italy

Abstract

Fused Deposition Modeling (FDM) finds extensive application across various fields due to its cost-effectiveness and user-friendly nature. However, it does come with certain limitations, including challenges in achieving high surface quality, precise dimensional tolerance, and the characteristic anisotropic mechanical properties it exhibits.
The aim of this paper is to investigate the machinability of 3D-printed PETG and analyze the roughness and burr formation that occurs as a result. A Design of Experiments (DoE) was developed with three factors: rotational speed, feed rate, and depth of cut. Each factor had different levels: rotational speed at 3000, 5500, and 8000 rpm; feed rate at 400, 600, and 800 mm/min; and depth of cut at 0.2, 0.4, 0.6, and 0.8 mm. The machinability was evaluated based on two response parameters: roughness (Sa), determined on the milled surface, and burr height, measured using a profilometer on both sides of the milled surface. The findings indicate that milling parameters strongly affect roughness and burr formation. However, the optimal conditions for minimizing roughness and burr formation are not coincident. The results were also compared to the machinability of PLA machined under similar conditions.

Peer-review under responsibility of the scientific committee of the 5th International Conference on Industry 4.0 and Smart Manufacturing

Keywords: PETG; 3D printing; milling; burr formation; surface quality; Design of Experiments; anisotropy;

1. Introduction

Additive Manufacturing (AM) technology has significantly expanded its applications in the industrial field, particularly in recent decades [1-3]. Within the context of Industry 4.0, 3D printing plays a crucial role by enabling

* Corresponding author. Tel.: +39 070 675 5721; fax: +39 070 675 5717.
E-mail address: m.elmehtedi@unica.it

Peer-review under responsibility of the scientific committee of the 5th International Conference on Industry 4.0 and Smart Manufacturing
10.1016/j.procs.2024.01.119

the production of parts with complex geometries at a relatively low cost. This technology offers rapid processes and reduces the production of scrap, which is commonly associated with conventional manufacturing production [4].

There are various types of 3D printing technologies, one of which is Fused Deposition Modeling (FDM), also known as Fused Filament Fabrication (FFF). In this technique, a thermoplastic filament is melted, extruded and deposited layer by layer to fabricate a three-dimensional object.

Numerous researchers have conducted extensive investigations into the mechanical properties of FDM 3D-printed samples [5–7]. It is well-known that the anisotropy of these samples is highly affected by the printing direction. This is due to the layer-by-layer construction method, where the bonding between layers is typically not as strong as the material itself. As a results, interlayer bonding can be weaker compared to intralayer bonding.

Every printing variable significantly influences the mechanical properties of the samples. The mechanical properties strongly depend on printing conditions such as the grid-type [8], infill density, and layer height [9]. Additional fibers in the filament and post-processing heat treatment [10] can be used to improve these properties. While PLA and ABS are the most commonly used materials in FDM technology, there is a growing interest in PETG due to its unique characteristics. PETG is an amorphous thermoplastic material derived from the copolymerization of Polyethylene Terephthalate, a homopolymer. It can be extruded as a filament for 3D printing (3DP) applications. PETG possesses exceptional mechanical characteristics and properties, including machinability, toughness, impact resistance, and brightness. Consequently, PETG is widely utilized in specific high-end applications. Compared to other 3D printable materials, PETG is known for its durability and relatively high strength. It is resistant to elevated temperatures, UV rays, and is hydrophobic [11].

Durgashyam et al. [12] have conducted a study on the influence of printing parameters on the mechanical properties of 3D printed PETG, demonstrating that parameters such as infill density, feed rate, and layer thickness have a significant impact on the tensile strength of the material. Lower layer thickness and higher infill density result in an increased tensile strength.

Surface quality is also greatly affected by printing parameters, as indicated by various authors [13–15]. Barrios and Romero [11] specifically investigated the impact of printing parameters on the surface quality of 3D printed PETG. The parameters they investigated included layer height, print temperature, print speed, print acceleration, and flow rate. The results suggested that the flow rate and print acceleration have the greatest influence on surface quality.

Based on these considerations, it becomes evident that FDM technology has certain limitations concerning surface quality, dimensional tolerance, and mechanical properties. To improve the quality surface several authors [1,16-19] propose post-printing solutions, as reported in Table 1.

Table 1 – Different post-printing solutions for enhancing the surface quality of 3D-Printed FDM parts.

	Post-process type	Material	Investigated parameters
Lalehpour et al. [16]	Acetone vapour bath	ABS	Roughness
Pandey et al. [17]	Hot cutter	ABS	Roughness
Pămărac et al. [18]	Milling	PLA and ABS	Roughness
Lalegani et al. [19]	Milling	PLA	Roughness
El Mehtedi et al. [1]	Milling	PLA	Roughness and burr formation

This paper represents a continuation of the research initiated in 2022, with a specific focus on the machinability of 3D-printed parts produced using FDM technology [1]. It has been demonstrated by other authors [18-21] that milling can be employed as a technique to enhance the surface quality of such samples. However, despite extensive research on materials like PLA and ABS, there remains a notable absence of experimentation aimed to enhance surface quality through milling operations in 3D-printed PETG. The present work concentrates on exploring the possibilities of improving the surface quality and understanding the machinability of 3D-printed Polyethylene Terephthalate Glycol (PETG) samples. The study investigates the influence of the main process parameters, namely rotational speed, feed rate, and depth of cut, on surface roughness and burr formation. By varying these parameters, a comprehensive understanding of their impact is achieved. An ANOVA test, conducted using Minitab software, helps determine which parameter has the greatest influence on the machining process. Additionally, the mechanical properties of the 3D-

printed samples have been evaluated in three printing directions. Furthermore, a comparison is made between the obtained results and those achieved under similar conditions for PLA. This comparative analysis provides valuable insights into the performance and characteristics of PETG in relation to PLA. Through this research, significant strides are made towards improving the surface quality and understanding the machinability of 3D-printed PETG samples, contributing to the existing knowledge in this field. In the following paragraphs, the experimental procedure and results will be discussed.

2. Experimental procedures

The printing material used in this study was PETG filament manufactured by Soitech. The manufacturer's recommended extrusion temperature of 250°C and printing bed temperature of 70°C. The project's mesh and g-code file were created using the open-source software FREECAD.

The TRONXY 5SA FDM printer, equipped with a 0.4 mm extruder, was employed for the printing process. To enhance adhesion on the printer bed, lacquer spray was applied.

The specimens for tensile test and milling machine's geometry, printed using the same printing parameters, are shown in Figure 1. The geometry of the samples is the same used in the previous study [1], facilitating better comparability of the results.

As already mentioned, the printing conditions followed the manufacturer's recommendations. The tensile test samples were printed following the UNE 116005:2012 standard in three directions: X, Y, and Z (Figure 1c). This standard was chosen due to its superior repeatability compared to other standards [22]. Tensile tests were carried out at room temperature to assess the mechanical properties of the printed PETG samples. The tests were conducted using a Galdabini SUN500 servo-electric machine equipped with a 5 kN load cell. A strain measurement was performed over a gauge length of 50 mm using an HBM DD1 Displacement Transducer. Three replications were conducted for each printing direction.

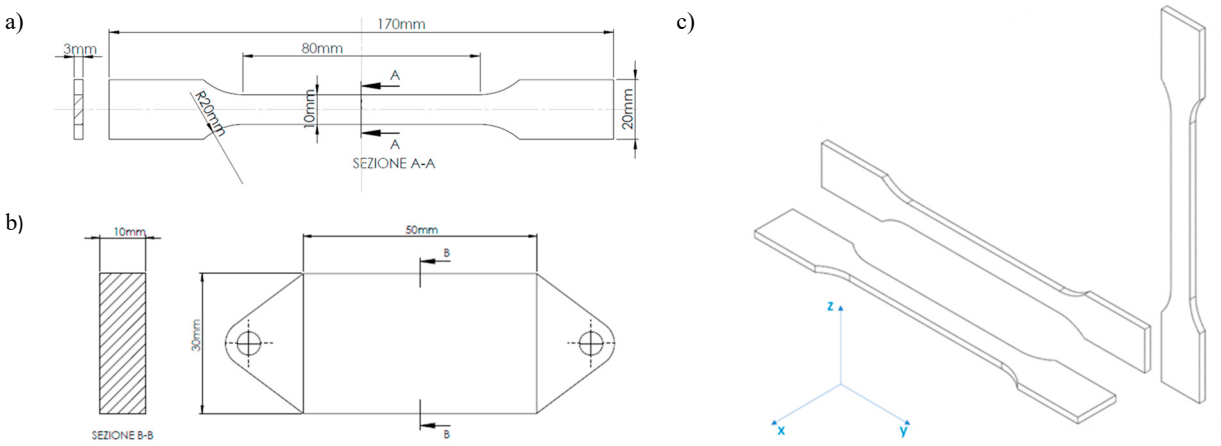

Fig. 1. (a) Tensile sample dimensions, (b) machining sample dimensions, and (c) Printing direction for tensile samples. [1]

A Design of Experiments (DoE) was developed to facilitate the execution of the milling experiment. For this purpose, a full factorial design was selected, which encompasses three factors: rotational speed (n), feed rate (Vf), and depth of cut (ap). These factors were chosen to conduct the milling operations effectively, and their corresponding values are reported in Table 1.

The milling experiments were carried out using a CNC3018 machine, equipped with a commercial milling tool (Master 660C). The execution of the experiment was randomized to ensure unbiased results. The Vectric Aspire software was used for the milling project, while the GRBL Control opensource controller was employed to control the CNC speed. Throughout the milling process, coolant was applied to ensure optimal conditions.

Table 2. Design of the Experiment, Factors' summary table.

Factors				Levels			
Name	Type	Units	Symbols	1	2	3	4
Rotational speed (n)	Numeric	[rpm]	A	3000	5500	8000	-
Feed Rate (Vf)	Numeric	[mm/min]	B	400	600	800	-
Depth of cut (ap)	Numeric	[mm]	C	0.2	0.4	0.6	0.8

The surface roughness evaluation involved measuring a 6 x 4 mm^2 area (as depicted in Figure 2), for each milled condition using the Taylor Hobson Ultra 2 roughness meter with a 50 mm stylus. Subsequently, the acquired surface data was processed using Talymap silver software. The Sa parameter was employed to describe the surface quality using Eq(1).

$$S_a = \frac{1}{A}\iint_A |S(x,y)|dxdy \quad (1)$$

To evaluate the height of the burr at both sides of each milling surface, three profile measurements were taken perpendicular to the milling direction, spaced equidistantly at 10 mm intervals. The measurements of the burr height were processed in Matlab using the least-squares method to establish a zero line, providing a reference level for accurate evaluation, similar to the method employed in [1]. Each measurement was divided into five zones: the unmilled surface zones were utilized to evaluate a regression line based on points without a burr, and the burr's height was calculated by subtracting the coordinate of the highest point on the burr from the corresponding coordinate on the regression line.

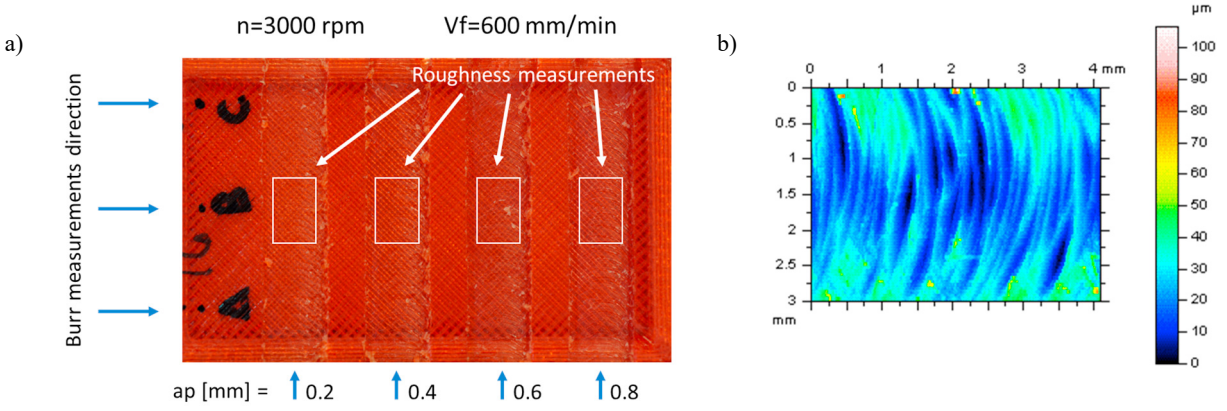

Fig. 2. (a) Sample machined showing the three Burr' measured directions; (b) Example surface roughness measurement Sa (in µm).

3. Results and discussion

3.1. Tensile test results

Nominal stress-strain curves for every tested sample are presented in Figure 3. From the recorded applied load and measured strain during the test, the Young modulus (E), Ultimate Tensile Strength (UTS), and Elongation at break (A%) were evaluated. These calculated values are reported in Table 2.

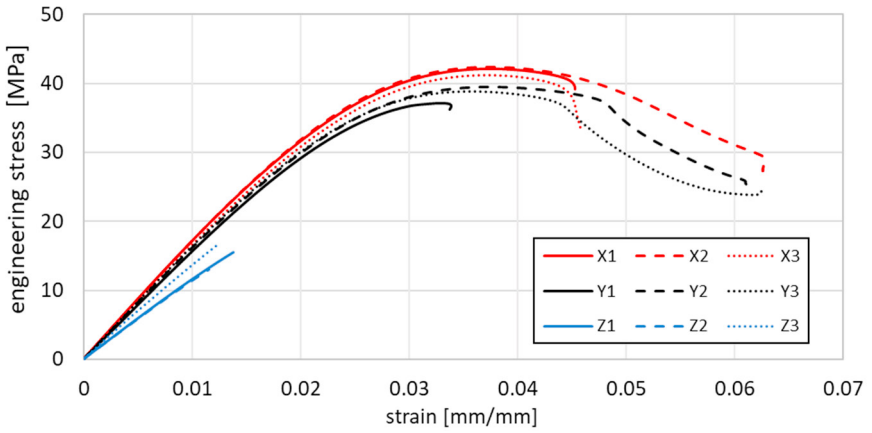

Fig. 3. Engineering stress vs. Engineering strain for all tested samples.

The results of the tensile tests demonstrate that the mechanical properties varied depending on the printing direction. The X printing direction stood out by exhibiting the highest mechanical properties among the three directions examined. This outcome suggests that the X direction provides better interlayer bonding and improved the mechanical performance compared to the other directions. The Y direction, on the other hand, showed mechanical properties similar to those of the X direction, indicating that it is also a viable printing direction for achieving desirable mechanical performance. In contrast, the Z direction displayed poor mechanical properties compared to both the X and Y directions. This finding can be attributed to the inherent challenges associated with achieving strong interlayer bonding in the vertical direction. In FDM technology, the layers are built up vertically, and ensuring proper adhesion and bonding between layers in the Z direction can be more difficult. As a result, the Z printing direction exhibited lower mechanical properties, including reduced strength, stiffness, and elongation at break. Importantly, these findings regarding the mechanical properties in different printing directions are consistent with previous research conducted by other authors [23], specifically regarding the mechanical properties in the X printing direction.

Table 3. presents the mechanical properties of 3D-printed PETG under various conditions. Additionally, a comparison is made with the mechanical properties obtained by Mahesh et al. [23].

printing directions	E [MPa]	σ_{UTS} [MPa]	A%
X	1661.1 ± 30.4	41.9 ± 0.6	5.1 ± 1.0
Y	1560.8 ± 34.1	38.5 ± 1.2	5.3 ± 1.6
Z	1233.4 ± 126.2	15.0 ± 1.8	1.3 ± 0.1
X [23]	1768.1 ± 15.9	51.9 ± 2.3	-

3.2. ANOVA Analysis for Sa

The measured surfaces were processed using Talymap Silver software, and the Sa parameter was recorded for each condition, as mentioned earlier. The range of variability for Sa was observed to be between 3.46 µm and 8.79 µm for the 5500 rpm, 400 mm/min, 0.2 mm condition and the 5500 rpm, 800 mm/min, 0.4 mm condition, respectively. These

values were subsequently analyzed using Minitab to evaluate the significance of each factor on the surface quality. A p-value of 0.05 was set as the threshold for relevance.

The Pareto Chart, depicted in Figure 4, presents the parameters in order of their statistical significance. The chart clearly indicates that the rotational speed (A), feed rate (B), and depth of cut (C) parameters, as well as their combinations, have a statistically significant influence on the response, with the exception of the (AC) combination. Among these parameters, it was determined that the feed rate had the most substantial impact on the overall process.

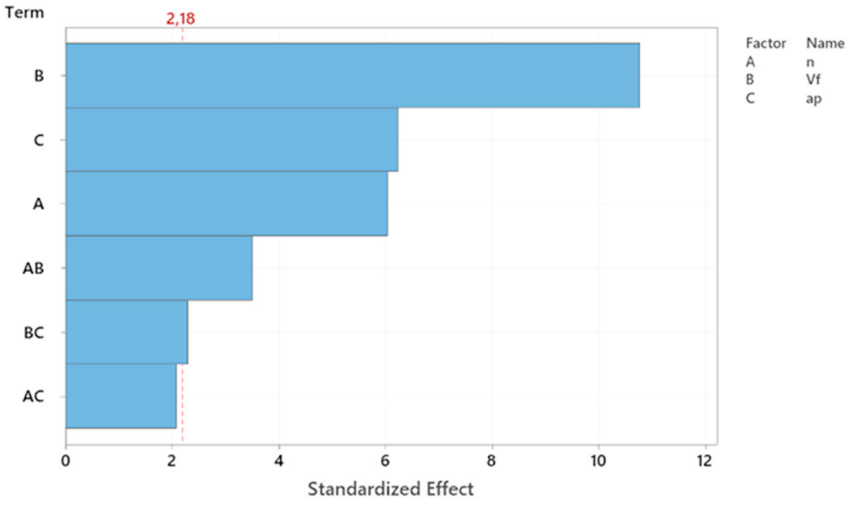

Fig. 4. Pareto Chart for Sa (α=0.05).

The main effect plot for Sa is illustrated in Figure 5, highlighting the relationship between the different factors and the roughness of the milled surface. It is evident from the plot that increasing the rotational speed leads to a decrease in roughness, whereas increasing the feed rate and depth of cut results in an increase in roughness.

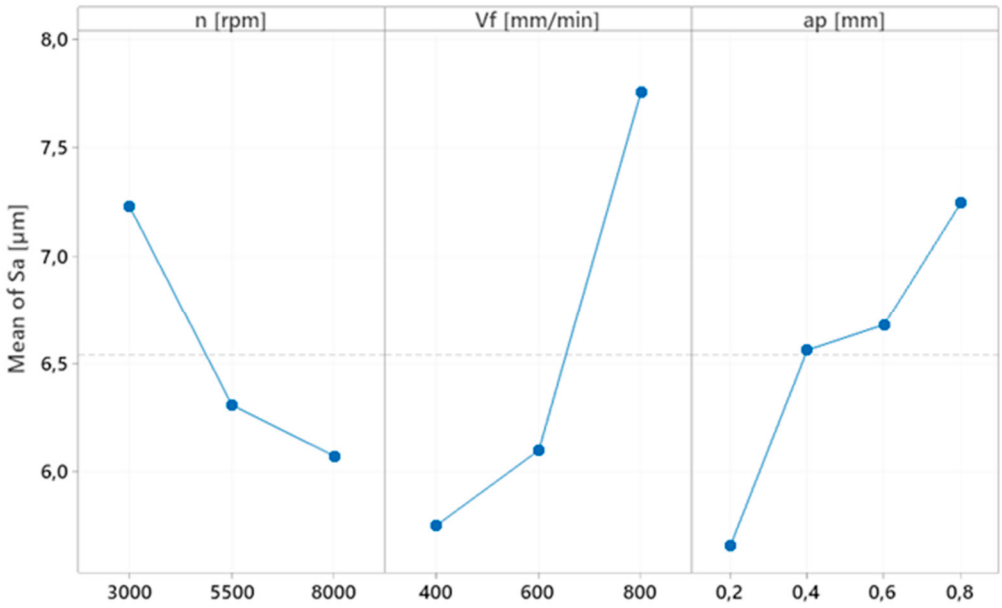

Fig. 5. Main effect plot for Sa (in µm).

3.3. Response for burr height

As mentioned earlier, the formation of burrs was evaluated on both sides of the milled surface, with three measurements conducted for each condition. An ANOVA test was performed on the burr height response, considering the mean values from both sides, and incorporating three replicates. The results for the burr height are shown in Figures 6 and 7.

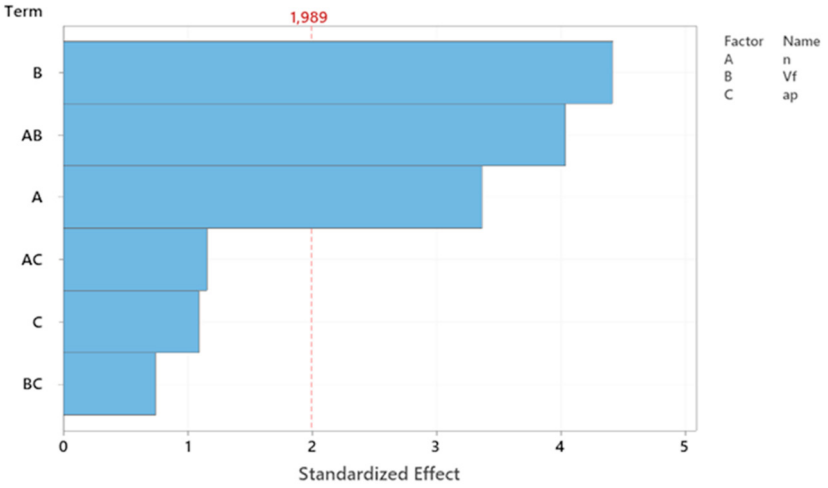

Fig. 6. Pareto Chart for burr formations (α=0.05).

The Pareto Chart depicted in Figure 6 reveals that only three parameters have a statistically significant influence on the process, ranked in order of their impact: feed rate (B), the combination of feed rate and rotational speed (AB), and rotational speed (A). The main effect plot for burr height is displayed in Figure 7, highlighting the relationship between the process parameters and the height of the burr within the studied range. The plot clearly indicates that increasing all process parameters results in a decrease in burr height. However, it is worth noting that at the highest levels of feed rate and depth of cut, there is a slight increase in burr height.

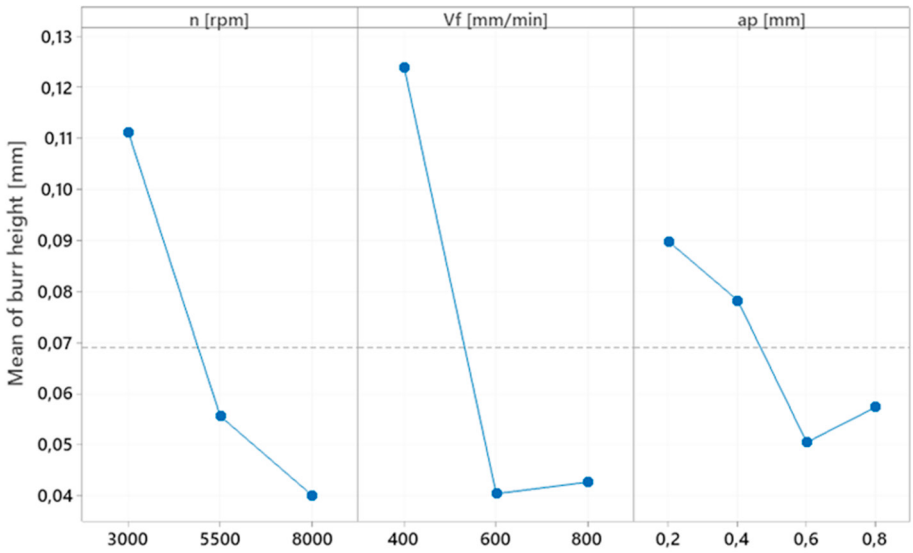

Fig. 7. Main effect plot for burr formation (in mm).

3.4. Discussion

In summary, in the range studied, it is clear that to reduce burr formation it would be appropriate to work at high levels of each parameter. Conversely, achieving a smoother surface implies milling at lower feed rates and depths of cut, along with higher rotational speeds. Consequently, the optimal settings for minimizing burr formation and surface roughness are distinct and exhibit an inverse relationship. While reducing burr formation requires working with higher parameter levels in the studied range, attaining a low roughness value necessitates lower feed rates and depths of cut but higher rotational speeds. Thus, achieving the desired results for both burr formation and surface roughness in the machining process requires a delicate balance between these parameters.
For example, if the purpose is to improve the quality surface of the 3D-printed part, lower feed rate and depth of cut is necessary, taking into account that the burr formation is higher in this condition and an additional process to remove the burr could be necessary. Another implication is that the total process time is affected, since lower Vf and ap means also lower material removing per time and additional time to remove the burr after the milling process.

3.5. Comparison of Machinability between PLA and PETG

Figure 8 illustrates a comparison of the machinability between PETG and PLA, utilizing results obtained from a previous study conducted in 2022 [1]. In the previous study, roughness along a line at the center of the milled surface was evaluated for PLA using the Ra parameter. In contrast, this current study utilized the Sa parameter to assess roughness across the surface of PETG, providing a more accurate estimation. The comparison reveals that the Sa values for PETG ranged from 3.46 µm to 8.79 µm, while the Ra values for PLA ranged from 2 µm to 13 µm.

In Figure 8a, it is evident that both materials exhibit a similar response trend for each factor. The roughness increases with an increase in feed rate and depth of cut for both materials. However, rotational speed does not have a significant effect on PLA and shows a minimum value at 5500 rpm, whereas a decreasing trend is observed for PETG.

Figure 8b presents a comparison of the results obtained for the burr height response. The same method was employed to evaluate burr height in both cases. To achieve a lower burr height, higher feed rate and depth of cut are found to be suitable for both materials. However, the effect of rotational speed on burr height differs between the two materials. PETG demonstrates a notable decrease in burr formation as the rotational speed is increased to higher levels. In other words, higher rotational speeds tend to suppress the formation of burrs in PETG. On the contrary, PLA exhibits a different behavior. The burr height for PLA reaches a minimum value at the medium level of rotational speed, suggesting that excessively high or low rotational speeds may result in increased burr formation for PLA.

The burr height is typically higher in PLA material compared to PETG when subjected to the same process parameters. This difference in burr height can be attributed to the variation in glass transition temperature between PLA (55°C) and PETG (75°C).

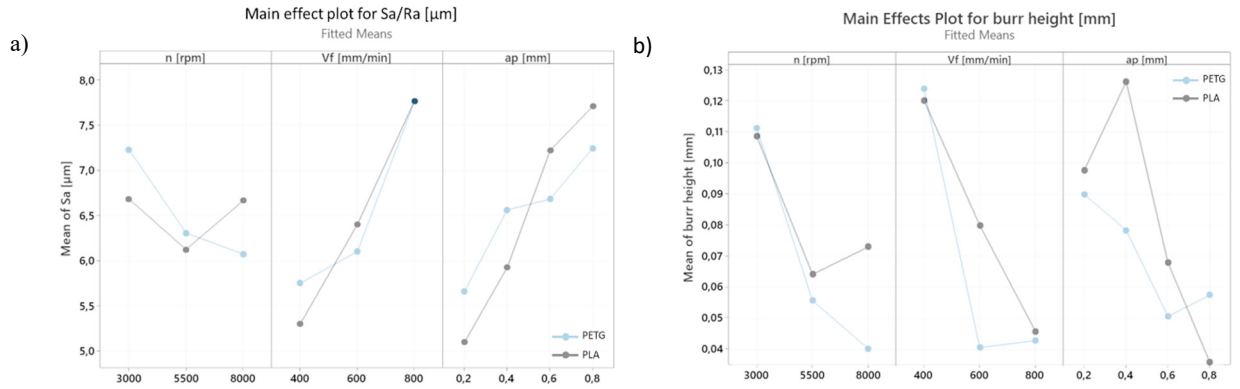

Fig. 8. Comparison of roughness (a) and burr height (b) main effect plot for PLA and PETG.

The lower glass transition temperature of PLA makes it more susceptible to deformation and material flow during the machining process, potentially resulting in increased burr formation. In contrast, the higher glass transition temperature of PETG provides better resistance to deformation and may contribute to reduced burr formation. Overall, it is evident that minimizing burr formation requires operating at higher levels of each parameter. On the other hand, minimizing roughness necessitates milling the surface at lower feed rates and depths of cut, but higher rotational speeds. As a result, the minimum values for burr formation and roughness responses are different and exhibit an opposite relationship. While minimizing burr formation requires operating at higher levels of each parameter, achieving a low roughness value necessitates lower feed rates and depths of cut but higher rotational speeds. Therefore, a careful balance between these parameters is essential to optimize the machining process and achieve the desired outcomes for both burr formation and surface roughness.

4. Conclusions

This paper aimed to investigate the machinability of 3D-printed PETG by focusing on the aspects of roughness and burr formation. The mechanical properties of the 3D-printed PETG samples were found to be similar with those reported in previous studies, reinforcing the reliability of the findings.

Through the implementation of a Design of Experiments (DoE), the study explored the influence of three operational factors (feed rate, depth cut, and rotational speed) at different levels on the machinability of PETG. The evaluation of machinability was based on two critical response parameters: roughness and burr height. The results demonstrate that the milling parameters significantly impact both roughness and burr formation. However, it is important to note that the optimal conditions for minimizing roughness and burr formation differ. Within the range studied, it was observed that reducing burr formation requires operating each parameter at higher levels. This indicates that increased cutting parameters can effectively minimize the occurrence of burrs during the machining process. On the other hand, minimizing surface roughness involves milling at lower feed rates and depth cuts, coupled with higher rotational speeds. These findings highlight the significance of carefully balancing the machining parameters to achieve the desired outcomes in terms of both roughness and burr formation.

Furthermore, a comparison with the machinability of 3D-printed PLA provided valuable insights into the contrasting characteristics of the two materials. The research outcomes presented in this study contribute to a comprehensive understanding of the machinability of 3D-printed PETG, thus facilitating informed decision-making and optimization of the machining process in practical applications. Milling operations have been examined in the simple context of the face milling process, but further research is required to gain a deeper understanding when dealing with contour milling and more complex geometries. Additionally, the influence of many parameters like tool geometry or printing orientation has not been taken into account and must be studied in future research.

References

[1] El Mehtedi, Mohamad, Buonadonna, Pasquale, Carta, Mauro, El Mohtadi, Rayane, Marongiu, Gianluca, Loi, Gabriela, and Aymerich, Francesco (2022) “Effects of milling parameters on roughness and burr formation in 3D- printed PLA components.” Procedia Computer Science 10.

[2] Boparai, Kamaljit Singh, Singh, Rupinder, and Singh, Harwinder (2016) “Development of rapid tooling using fused deposition modeling: a review.” Rapid Prototyping Journal **22** (**2**): 281–299.

[3] Clini, Paolo, El Mehtedi, Mohamad, Nespeca, Romina, Ruggeri, Ludovico, and Raffaelli, Elisa (2018) “A digital reconstruction procedure from laser scanner survey to 3d printing: the theoretical model of the Arch of Trajan (Ancona).” SCIRES-IT – SCIentific RESearch and Information Technology **7** (**2**): 1–12.

[4] Wang, Xin, Jiang, Man, Zhou, Zuowan, Gou, Jihua, and Hui, David (2017) “3D printing of polymer matrix composites: A review and prospective.” Composites Part B: Engineering **110** 442–458.

[5] Mansour, M., Tsongas, K., Tzetzis, D., and Antoniadis, A. (2018) “Mechanical and Dynamic Behavior of Fused Filament Fabrication 3D Printed Polyethylene Terephthalate Glycol Reinforced with Carbon Fibers.” Polymer-Plastics Technology and Engineering **57** (**16**): 1715–1725.

[6] M, Vinyas, J, Athul S, D, Harursampath, and T, Nguyen Thoi (2019) “Mechanical characterization of the Poly lactic acid (PLA) composites prepared through the Fused Deposition Modelling process.” Materials Research Express **6** (**10**): 105359.

[7] Rodríguez-Panes, Adrián, Claver, Juan, and Camacho, Ana (2018) “The Influence of Manufacturing Parameters on the Mechanical Behaviour of PLA and ABS Pieces Manufactured by FDM: A Comparative Analysis.” Materials **11** (**8**): 1333.

[8] Srinidhi, M.S., Soundararajan, R., Satishkumar, K.S., and Suresh, S. (2021) "Enhancing the FDM infill pattern outcomes of mechanical behavior for as-built and annealed PETG and CFPETG composites parts." Materials Today: Proceedings **45** 7208–7212.

[9] Ajay Kumar, M., Khan, M.S., and Mishra, S.B. (2020) "Effect of machine parameters on strength and hardness of FDM printed carbon fiber reinforced PETG thermoplastics." Materials Today: Proceedings **27** 975–983.

[10] Bhandari, Sunil, Lopez-Anido, Roberto A., and Gardner, Douglas J. (2019) "Enhancing the interlayer tensile strength of 3D printed short carbon fiber reinforced PETG and PLA composites via annealing." Additive Manufacturing **30** 100922.

[11] Barrios, Juan M., and Romero, Pablo E. (2019) "Improvement of Surface Roughness and Hydrophobicity in PETG Parts Manufactured via Fused Deposition Modeling (FDM): An Application in 3D Printed Self–Cleaning Parts." Materials **12** (**15**): 2499.

[12] Durgashyam, K., Indra Reddy, M., Balakrishna, A., and Satyanarayana, K. (2019) "Experimental investigation on mechanical properties of PETG material processed by fused deposition modeling method." Materials Today: Proceedings **18** 2052–2059.

[13] Kovan, V, Tezel, T, Topal, E.s, and Camurlu, H.e (2018) "Printing parameters effect on surface characteristics of 3d printed pla materials." Machines. Technologies. Materials. **12** (**7**): 266–269.

[14] Vidakis, Nectarios, David, Constantine, Petousis, Markos, Sagris, Dimitrios, Mountakis, Nikolaos, and Moutsopoulou, Amalia (2022) "The effect of six key process control parameters on the surface roughness, dimensional accuracy, and porosity in material extrusion 3D printing of polylactic acid: Prediction models and optimization supported by robust design analysis." Advances in Industrial and Manufacturing Engineering **5** 100104.

[15] Vasudevarao, Bharath, Natarajan, Dharma Prakash, and Henderson, Mark "Sensitivity of Rp surface finish to process parameter variation." 9.

[16] Lalehpour, Amirali, and Barari, Ahmad (2016) "Post processing for Fused Deposition Modeling Parts with Acetone Vapour Bath." IFAC-PapersOnLine **49** (**31**): 42–48.

[17] Pandey, Pulak M, Reddy, N Venkata, and Dhande, Sanjay G (2003) "Improvement of surface finish by staircase machining in fused deposition modeling." Journal of Materials Processing Technology 9.

[18] Pămărac, Răzvan Gabriel, and Petruse, Radu Emanuil (2018) "Study Regarding the Optimal Milling Parameters for Finishing 3D Printed Parts from ABS and PLA Materials." ACTA Universitatis Cibiniensis **70** (**1**): 66–72.

[19] Lalegani Dezaki, Mohammadreza, Mohd Ariffin, Mohd Khairol Anuar, and Ismail, Mohd Idris Shah (2020) "Effects of CNC Machining on Surface Roughness in Fused Deposition Modelling (FDM) Products." Materials **13** (**11**): 2608.

[20] Vallejo, J., García-Plaza, E., Núñez, P. J., Chacón, J. M., Caminero, M. A., and Romero, A. (2023) "Machinability analysis of carbon fibre reinforced PET-Glycol composites processed by additive manufacturing." Composites Part A: Applied Science and Manufacturing **172** 107561.

[21] Bruni, C., Gianangeli, C., Mancia, T., Greco, L., and Pieralisi, M. (2020) "Improving dimensional and surface quality of additive manufactured parts." Journal of Physics: Conference Series **1507** (**4**): 042003.

[22] García-Domínguez, Amabel, Claver, Juan, Camacho, Ana María, and Sebastián, Miguel A. (2020) "Considerations on the Applicability of Test Methods for Mechanical Characterization of Materials Manufactured by FDM." Materials **13** (**1**): 28.

[23] Mahesh, Vinyas, Joseph, Athul S., Mahesh, Vishwas, Harursampath, Dineshkumar, and Vn, Chethan (2021) "Investigation on the mechanical properties of additively manufactured PETG composites reinforced with OMMT nanoclay and carbon fibers." Polymer Composites **42** (**5**): 2380–2395